

Synchronization in Networks of Hindmarsh–Rose Neurons

Paolo Checco, *Member, IEEE*, Marco Righero, *Student Member, IEEE*, Mario Biey, and Ljupco Kocarev, *Fellow, IEEE*

Abstract—Synchronization is deemed to play an important role in information processing in many neuronal systems. In this work, using a well known technique due to Pecora and Carroll, we investigate the existence of a synchronous state and the bifurcation diagram of a network of synaptically coupled neurons described by the Hindmarsh–Rose model. Through the analysis of the bifurcation diagram, the different dynamics of the possible synchronous states are evidenced. Furthermore, the influence of the topology on the synchronization properties of the network is shown through an example.

Index Terms—Bifurcation, biological systems, networks, nonlinear oscillators, synchronization.

I. INTRODUCTION

DURING the last few years networks of bio-inspired neurons have interested an increasing number of researchers in all branches of science. In particular, spiking neurons have attracted the interest because many studies consider this behavior an essential component in information processing by the brain [1]. In this class of neurons, bursting neurons are of relevant interest since they characterize a variety of biological oscillators. The electrical potential of these neurons, which typically is the state variable that contains the main information, undergoes a succession of alternating active and silent phases in which, respectively, it has a spiking behavior (very fast oscillations) and it evolves slowly without oscillations. Furthermore, the notion of synchronization is related to several central issues of neuroscience [2]; synchronization seems to be a central mechanism for neuronal information processing within a brain area as well as for communication between different brain areas. For example, synchronization between areas of the visual cortex and parietal cortex, and between areas of the parietal and motor cortex was observed during the visual-motor integration task in awake cats [3]. Direct participation of synchrony in a cognitive task was experimentally demonstrated in humans [4]. This motivates the investigation of the conditions for synchronization in networks of bursting neurons [5], [6]. Among many simple bursting models, the Hindmarsh–Rose (HR) neuron [7] is fairly simple and popular. It is described by a system of three coupled first-order differential equations in which the first state variable

shows the succession of alternating active and silent phases. The synchronization conditions of a network of HR neurons have been studied in several papers (for example see [5], [6], [8]) and more detailed conditions have been recently introduced in [9], [10].

In this paper we focus on a network of synaptically coupled HR neurons and we derive its synchronization conditions, resorting to the well established technique proposed by Pecora and Carroll [11]. As a first result of our investigation, using the above-mentioned technique, the approximate results given in [6] are retrieved and their limits are evidenced. Furthermore, it turns out that the synchronous behavior may be different from that of an isolated neuron and it has to be evaluated resorting to a time-domain analysis, using the coupling strength as bifurcation parameter. Hence, the second aim of this paper is to give a complete analysis of the possible synchronous states by determining the corresponding bifurcation diagram. Finally, it will be shown that the synchronization properties still depend—even if not strongly—on the topology of the network.

II. PRELIMINARIES

The HR neuron model [7]—originally proposed to model the synchronization of firing of two snail neurons [12]—can be generalized as follows [13], [14]:

$$\begin{cases} \dot{x}(t) = y - F(x) + I - z + u \\ \dot{y}(t) = G(x) - y \\ \dot{z}(t) = (1/\tau)(H(x) - z) \end{cases} \quad (1)$$

where $x(t)$ represents the membrane potential, usually considered as the natural output of the cell, $y(t)$ and $z(t)$ are the recovery and the adaptation variables taking into account, respectively, fast and slow ion currents and dots denote time derivatives. The external stimulus is given by constant I and input u . Furthermore, τ is the time constant of the slow ion current and the functions $F(x)$, $G(x)$, and $H(x)$ are chosen to display the generation of bursts of spikes and are usually third-, second-, and first-order polynomials, respectively.

In view of a future comparison, let us use the same parameters as in [6], [8]: $F(x) = bx^2 - ax^3$, $G(x) = c - dx^2$, and $H(x) = s(x - x_1)$, where $a = 1$, $b = 2.8$, $c = 0$, $d = -4.4$, $s = 9$, $x_1 = -5/9$, $I = 0$, $\tau = 1000$, and, for an isolated cell, $u = 0$. It follows that the studied cells are described by the following equations:

$$\begin{cases} \dot{x}(t) = f_x(x, y, x) = 2.8x^2 - x^3 - y - z \\ \dot{y}(t) = f_y(x, y, x) = 4.4x^2 - y \\ \dot{z}(t) = f_z(x, y, x) = 0.001 [9(x + 5/9) - z]. \end{cases} \quad (2)$$

With the free parameters fixed at the chosen values, the time evolution of the state variables is periodic. The coupling in a

Manuscript received April 08, 2008; revised June 26, 2008. Current version published December 12, 2008. This work was supported in part by Ministero dell'Università e della Ricerca under PRIN Project 2006093814_003. This paper was recommended by Associate Editor Y. Horio.

P. Checco, M. Righero and M. Biey are with the Department of Electronics, Politecnico di Torino, 10129 Torino, Italy (e-mail: marco.righero@polito.it).

L. Kocarev is with the Institute of Nonlinear Science, University of California at San Diego, La Jolla, CA 92093 USA.

Digital Object Identifier 10.1109/TCSII.2008.2008057

network of N such neurons can be modeled in different ways. In this work we focus on synaptic coupling between the x variables. In the simplest case where time delays and internal variables can be neglected, the synaptic coupling is often approximated by a static sigmoidal nonlinear input-output function γ with a threshold and saturation [14]:

$$\gamma(x_j) = \frac{1}{1 + e^{-\nu(x_j - \theta_s)}}. \quad (3)$$

As in [6], the free parameters are chosen to be $\nu = 10$ and $\theta_s = -0.25$. The evolution of the i -th neuron of the network is ruled by

$$\begin{cases} \dot{x}_i(t) = f_x(x_i, y_i, x_i) - g_s \sigma(x_i) \sum_{j=1}^N a_{ij} \gamma(x_j) \\ \dot{y}_i(t) = f_y(x_i, y_i, x_i) \\ \dot{z}_i(t) = f_z(x_i, y_i, x_i) \end{cases} \quad (4)$$

where g_s is the coupling strength and a_{ij} are the elements of the *adjacency matrix* \mathbf{A} , defined as follows: $a_{ii} = 0$; $a_{ij} = a_{ji} = 1$ if neurons i and j are connected to each other, 0 otherwise. Furthermore, $\sigma(x_i) = x_i - V_s$, where V_s is the reversal potential, assumed to be $V_s = 2$. Letting $\xi_i = (x_i, y_i, z_i)^T$ and $\mathbf{f} = (f_x, f_y, f_z)^T$, where $(\cdot)^T$ denotes transpose, the above equations can be recast as follows:

$$\dot{\xi}_i = \mathbf{f}(\xi_i) - (x_i - V_s) \sum_{j=1}^N g_{ij} \Gamma(\xi_j) \quad (5)$$

where $\Gamma(\xi_j) = (\gamma(x_j), 0, 0)^T$ and $g_{ij} = g_s a_{ij}$ are the elements of the *weighted adjacency matrix* $\mathbf{G} = g_s \mathbf{A}$.

III. MODIFIED MASTER STABILITY FUNCTION

In order to obtain the conditions of identical synchronization, the *master stability equation/function* approach is used [11], because it permits to separate the contribute of the identical isolated cells and of the topology of the network in the synchronization conditions. It is important to remark that this approach permits to verify if the synchronous state is (locally) stable or not, that is if the state vector of the network, starting sufficiently close to the synchronous state, converges to it. By considering the identical synchronization conditions, i.e. $\xi_1 = \xi_2 = \dots = \xi_N = \xi^*$, it follows that the synchronous state exists only if the sum of g_{ij} is constant with respect to i , i.e. all the nodes have identical degree k [6]:

$$\sum_{j=1}^N g_{ij} = g_s \sum_{j=1}^N a_{ij} = g_s k. \quad (6)$$

The evolution of the synchronous state is then described by the following system of ordinary differential equations:

$$\dot{\xi}^*(t) = \mathbf{f}(\xi^*) - k g_s (x^* - V_s) \Gamma(\xi^*). \quad (7)$$

The *Master Stability Equation* (MSE) associated to (5) is (for details see [11], [15])

$$\dot{\zeta}(t) = \left(D\mathbf{f}(\xi^*) + \begin{pmatrix} -k g_s \gamma(x^*) & 0 & 0 \\ 0 & 0 & 0 \\ 0 & 0 & 0 \end{pmatrix} + (\alpha + \nu\beta) \begin{pmatrix} (x^* - V_s) \left[\frac{d\gamma}{dx}(x^*) \right] & 0 & 0 \\ 0 & 0 & 0 \\ 0 & 0 & 0 \end{pmatrix} \right) \zeta \quad (8)$$

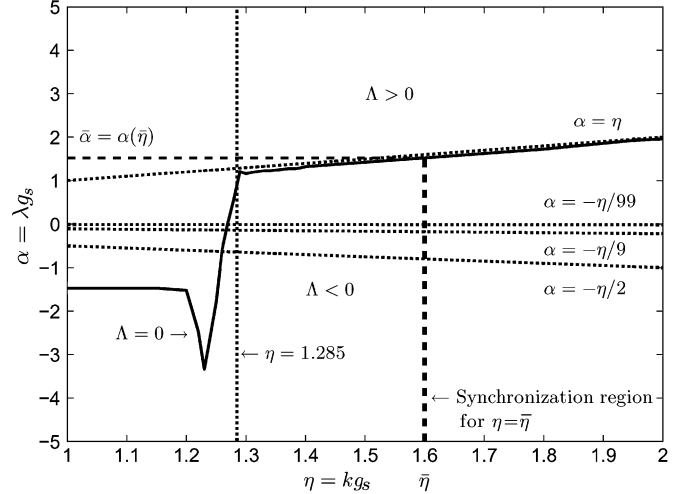


Fig. 1. Sign of the modified MSF with bounds on the second eigenvalue of \mathbf{G} (dotted lines) and synchronization region (dashed bold line) corresponding to $\eta = \bar{\eta}$.

where $D\mathbf{f}(\xi^*)$ is the Jacobian matrix of the function \mathbf{f} estimated on the synchronization manifold ξ^* , x^* is the first component of the synchronization manifold, $(d\gamma/dx)(x^*)$ is the derivative of $\gamma(x)$ with respect to x evaluated in x^* , and $\alpha + \nu\beta$ are the eigenvalues of the weighted adjacency matrix \mathbf{G} . The largest Lyapunov exponent $\Lambda = \Lambda(\alpha, \beta)$ of the MSE is known as the *Master Stability Function* (MSF) and it allows one to identify the synchronous conditions: the synchronous state is stable, i.e. the network synchronizes, if all the eigenvalues of the weighted adjacency matrix $\mathbf{G} = g_s \mathbf{A}$ (apart the largest one) lie in the so-called *synchronization region*, that is the region where the MSF $\Lambda(\alpha, \beta)$ is negative. In the case under investigation, \mathbf{G} is symmetric. It follows that its eigenvalues are real and both the MSE, (8), and the MSF do not depend on β , i.e. $\Lambda = \Lambda(\alpha)$. Furthermore, the eigenvalues of \mathbf{G} can be expressed as $g_s \lambda_i$, being λ_i a generic eigenvalue of the adjacency matrix \mathbf{A} . Differently from the original MSF [11], a global parameter related to the structure of the network can be identified in (7) and (8): the product between g_s and k . Defining $\eta = k g_s$, a *modified MSE* is obtained, which is hence a function of both α and η , namely $\Lambda = \Lambda(\alpha, \eta)$. Fig. 1 shows the curve where $\Lambda(\alpha, \eta) = 0$. It was obtained (a) by using the algorithm described in [16] to evaluate the largest Lyapunov exponent Λ of (8) as α and η varied, with $\beta = 0$, and (b) by determining the values of α and η for which $\Lambda(\alpha, \eta) = 0$ via a bisection method. It turns out that, for a given value $\bar{\eta}$ of η , the synchronization region is the vertical straight line below the curve $\Lambda = 0$, passing through the considered value $\bar{\eta}$ (dashed bold line in Fig. 1). This result is valid for other values of the neuron parameters as well. Hence, the considered networks of HR neurons are *Class-A networks* (see [15]): for a given value of $\eta = \bar{\eta}$, they synchronize if $g_s \lambda_2 < \bar{\alpha}$ where $\bar{\alpha} = \alpha(\bar{\eta})$ is the value of the $\Lambda = 0$ curve of Fig. 1 at $\eta = \bar{\eta}$, and λ_2 is the second largest eigenvalue of the adjacency matrix \mathbf{A} , whose spectrum is $\lambda_1 \geq \lambda_2 \geq \dots \geq \lambda_N$.

IV. SYNCHRONIZATION PROPERTIES

Thanks to the results obtained in the previous section, fixed a network, i.e. its topology (described by \mathbf{A}) and its coupling strength g_s , the synchronization conditions can be evaluated and

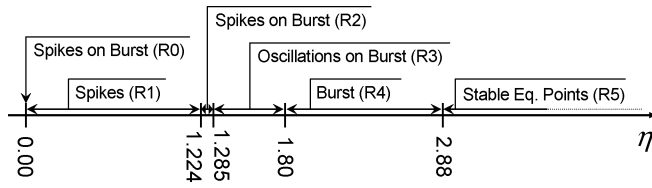


Fig. 2. Simplified bifurcation diagram, reporting only the attractors, of the synchronous state equation with respect to η parameter.

in this Section they will be investigated in details. Since we are dealing with class-A networks, the synchronous behavior is controlled by the second largest eigenvalue $g_s \lambda_2$. Hence, given an adjacency matrix \mathbf{A} and a coupling strength g_s , it is possible to predict the synchronization behavior of the network as follows: 1) compute the second eigenvalue λ_2 of \mathbf{A} and the row sum k ; 2) in Fig. 1, locate the synchronization region corresponding to the resulting value of $\eta = g_s k$. If the point $(g_s \lambda_2, g_s k)$ lies inside this region, then the network is expected to synchronize. Recall that the first eigenvalue λ_1 of \mathbf{A} is k , so the largest eigenvalue of \mathbf{G} is $g_s \lambda_1 = g_s k = \eta$, hence the straight line $\alpha = g_s k = \eta$ bounds the whole spectrum of \mathbf{G} from above. Moreover λ_2 , the second eigenvalue of \mathbf{A} , always satisfies the inequality (see [17]): $\lambda_2 \geq -k/(N-1)$, so the second eigenvalue of \mathbf{G} is always greater or equal to $-\eta/(N-1)$, where N is the number of neurons in the network. In Fig. 1, the straight lines $\alpha = \eta$ and $\alpha = -\eta/(N-1)$ for $N = 3, 10$ and 100 are superimposed (dotted lines) to the $\Lambda = 0$ curve. From this figure, it is easy to see that—to a good approximation—for $\eta > 1.285$ the second eigenvalue of \mathbf{G} is always in the stable region for every value of N and k , and hence, to a first approximation, synchrony does not depend on topology. This is coherent with [6], [8], where the estimated synchronization condition

$$g_s > g_s^c/k \quad (9)$$

is suggested, being $g_s^c = 1.285$ the critical value to get synchronization in a network composed of two mutually coupled neurons ($k = 1$). However, since the straight line $\eta = 1.285$ does not exactly coincide with the curve $\Lambda = 0$, for small N (3 or 4 for example) the limit to obtain stable synchronization can be a little lower. Hence, to a higher degree of approximation, we may expect that (i) synchronization is possible even for $\eta < 1.285$ and (ii) topology still influences synchronization to some extent. These interesting features will be highlighted in some of the examples of Section VI.

V. BIFURCATION DIAGRAM

In the case of synaptic coupling, the synchronous equation (7) is not equal to the equation of an isolated HR neuron (2) any more. Then, if the synchronization condition is verified, the state variables of all the cells synchronize, but the time evolution of the synchronous state is not known and depends on the parameter η , which accounts for coupling strength and cell degree [see (7)]. This fact motivates the investigation of the dynamic behavior when η is varied, i.e., of the bifurcation diagram with respect the parameter η . Using η as bifurcation parameter, we have thoroughly investigated the synchronous behavior by extensive numerical simulations of (7). Fig. 2 shows a simplified

version of the bifurcation diagram in which only a qualitative description of the attractors has been reported. By looking at the time evolution of the membrane potential $x(t)$ [see (1)], it was possible to identify five different types of attractors in five not overlapping intervals and one isolated point at $\eta = 0$. In the isolated point R0 ($\eta = 0$) and in R2 region [$\eta \in (1.224, 1.285)$] a spiking burst behavior is exhibited, i.e. there is a succession of two alternating phases (bursts) and the spikes are only in the active ones. Note that the point R0 corresponds to an isolated HR neuron. In R1 region [$\eta \in (0.00, 1.224)$] a spike behavior takes place. The synchronous behavior is composed of oscillations on bursts in region R3 [$\eta \in (1.285, 1.80)$]. The synchronous state exhibits a periodic behavior (only burst phases) in R4 region [$\eta \in (1.80, 2.88)$]. Finally, in R5 region the behavior reduces to a stable equilibrium point. It is worth pointing out that, due to results obtained in the previous Section, the behavior of region R1 can never be observed. This analysis reveals that one of the most interesting behaviors, the spiking on bursts, is reached in the windows between 1.224 and 1.285. Fig. 1 reveals that, for small networks, synchronization can be achieved even for these values of η .

As a final remark, let us stress that the results of this and the previous Sections were obtained for a broad range of values for α and η , i.e. are valid for different topologies and values of coupling strength. So Figs. 1 and 2 allow us to analyze a given network, saying whether it can synchronize or not and on which particular synchronous state. This will be illustrated in the examples of the following Section.

VI. EXAMPLES

As a first example, let us consider a network composed of just four HR neurons ($N = 4$), whose topology is described by the following adjacency matrix

$$\mathbf{A} = \begin{pmatrix} 0 & 1 & 0 & 1 \\ 1 & 0 & 1 & 0 \\ 0 & 1 & 0 & 1 \\ 1 & 0 & 1 & 0 \end{pmatrix} \quad (10)$$

from which $k = 2$, $\lambda_1 = 2$, $\lambda_{2,3} = 0$, and $\lambda_4 = -2$. If the coupling strength is $g_s = 0.50$, the η parameter is $\bar{\eta} = k g_s = 1.0$ and, from the $\Lambda = 0$ curve, $\bar{\alpha} = \alpha(\bar{\eta}) = -1.45$. It follows that the network cannot synchronize because $g_s \lambda_2 = 0 \not< \bar{\alpha} = -1.45$. Fig. 3 shows the time evolution of the first state variable of the first neuron and the global error $err(t)$, defined as

$$err(t) = \text{std}^2(\mathbf{x}(t)) + \text{std}^2(\mathbf{y}(t)) + \text{std}^2(\mathbf{z}(t)) \quad (11)$$

where $\text{std}(\cdot)$ is the standard deviation and $\mathbf{x}(t), \mathbf{y}(t), \mathbf{z}(t)$ are, respectively, the N -dimensional time-varying vectors of the first, second and third state variables of the N cells. In particular, $err(t) \rightarrow 0$ if and only if the cells synchronize on the same behavior. In this example the error does not converge to zero and hence the network does not synchronize, as predicted. On the other hand, if the coupling strength is increased to $g_s = 0.70$, the η parameter is $\bar{\eta} = k g_s = 1.40$ and, from the $\Lambda = 0$ curve, $\bar{\alpha} = \alpha(\bar{\eta}) = 1.30$. It follows that the network synchronizes because $g_s \lambda_2 = 0 < \bar{\alpha} = 1.30$. Furthermore, the synchronous behavior is composed of damped oscillations on

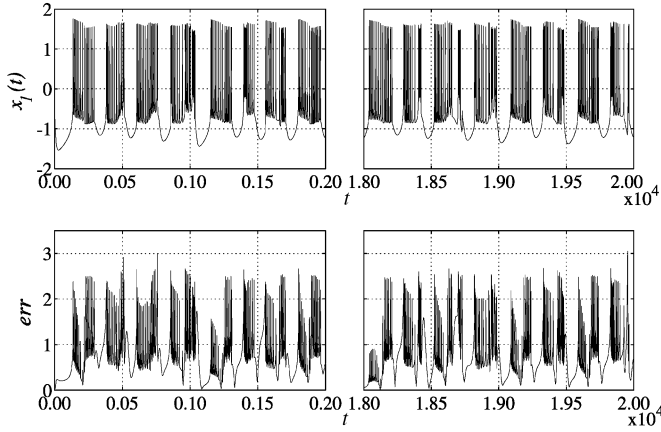


Fig. 3. Time evolution of the first state variable of the first neuron (upper) and (lower) of the network with $g_s = 0.50$ and adjacency matrix (10).

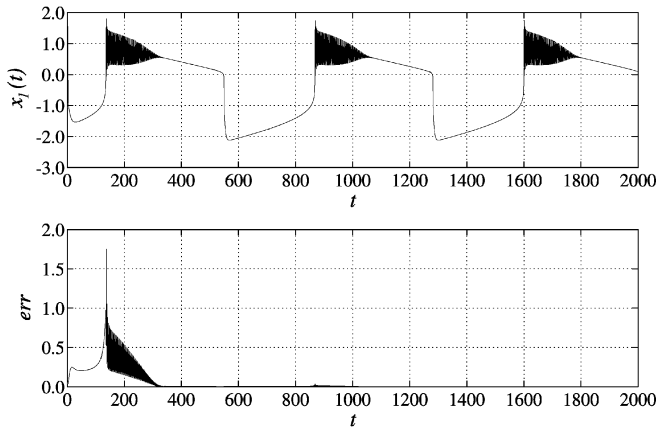


Fig. 4. Time evolution of the first state variable of the first neuron (upper) and global error (lower) of the network with $g_s = 0.70$ and adjacency matrix (10).

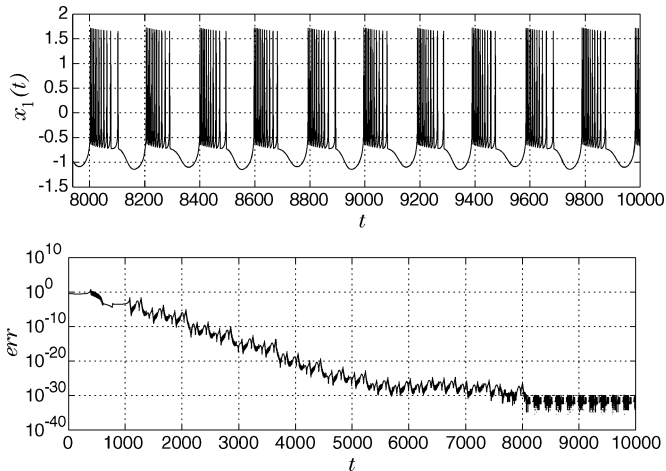


Fig. 5. Time evolution of the first state variable (upper, transient dropped off) and of the global error (lower) for a network of neurons with \mathbf{A} as in (12) and $g_s = 0.6305$.

burst, as described by the bifurcation diagram: $\bar{\eta} \in R3$. These results are confirmed by the simulations shown in Fig. 4.

As a second example, we consider a network which fails to satisfy the approximate condition (9) but satisfies the condition given by the MSF/MSE approach of Fig. 1. Consider a

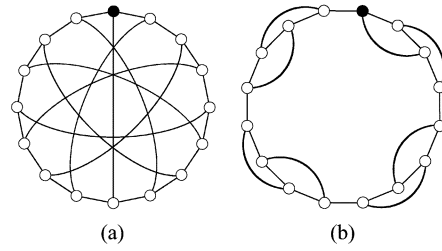


Fig. 6. Two networks belonging to the class $\mathfrak{N}(16, 3)$ with different topologies. The cells are numbered clockwise starting from the black one.

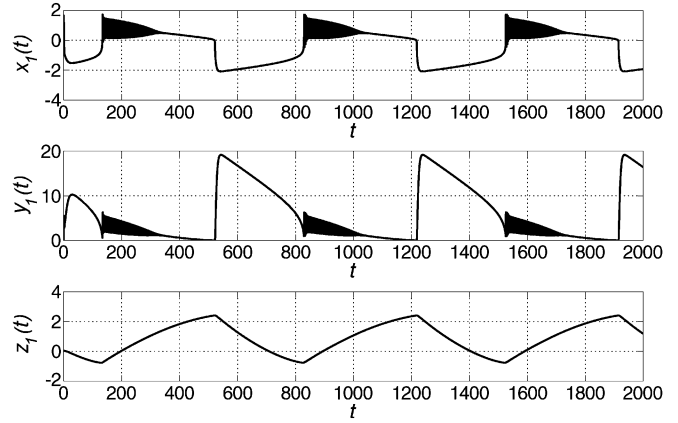


Fig. 7. State evolution of the cell 1 of the network whose topology is reported in Fig. 6(a).

network of three neurons mutually coupled in an all-to-all configuration, so that its adjacency matrix is

$$\mathbf{A} = \begin{pmatrix} 0 & 1 & 1 \\ 1 & 0 & 1 \\ 1 & 1 & 0 \end{pmatrix} \quad (12)$$

from which $k = 2$, $\lambda_1 = 2$ and $\lambda_{2,3} = -1$. With $g_s = 0.6305$, we have $\bar{\eta} = g_s k = 1.261 < 1.285$, and hence the approximated condition of (9), as it is a sufficient one, provides no information about the synchronization properties. On the contrary, the more precise criterion obtained from Fig. 1 gives $g_s \lambda_2 = -0.6395 < \alpha(\bar{\eta}) = -0.5917$ and hence this simple network should synchronize. Moreover, the bifurcation diagram predicts spikes on bursts as synchronous behavior. Numerical simulations of this network, shown in Fig. 5, confirm our forecast. As a last example, let us consider classes of networks of HR neurons $\mathfrak{N}(N, k)$ defined as the set of networks characterized by the same number of nodes N and the same node degree k and take the class $\mathfrak{N}(16, 3)$ and the coupling strength $g_s = 0.4287$. The $\bar{\alpha}$ value is estimated from the curve $\Lambda = 0$ of Fig. 1: $\bar{\alpha} \simeq 1.06$. It follows that a network synchronizes if and only if $g_s \lambda_2 < \bar{\alpha} \simeq 1.06$. Let us consider a first network belonging to $\mathfrak{N}(16, 3)$, characterized by the topology shown in Fig. 6(a): the adjacency matrix \mathbf{A} , not reported for lack of space, has been computed numbering clockwise the cells starting from the black one. The two largest eigenvalues of the associated adjacency matrix are $\lambda_1 = 3.0$, $\lambda_2 = 2.4142$. It follows that the considered network synchronizes because $g_s \lambda_2 \simeq 1.035 < \bar{\alpha} \simeq 1.06$. The evolution of the state variables of the cell 1 and the global error are reported, respectively, in Fig. 7 and Fig. 8: the states of

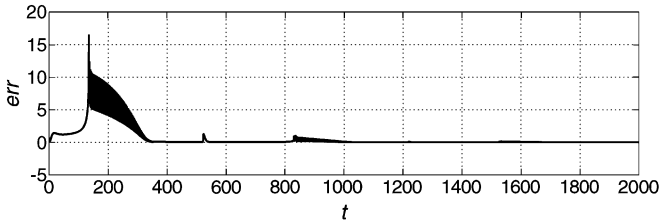


Fig. 8. Global error of the evolution of the network whose topology is reported in Fig. 6(a).

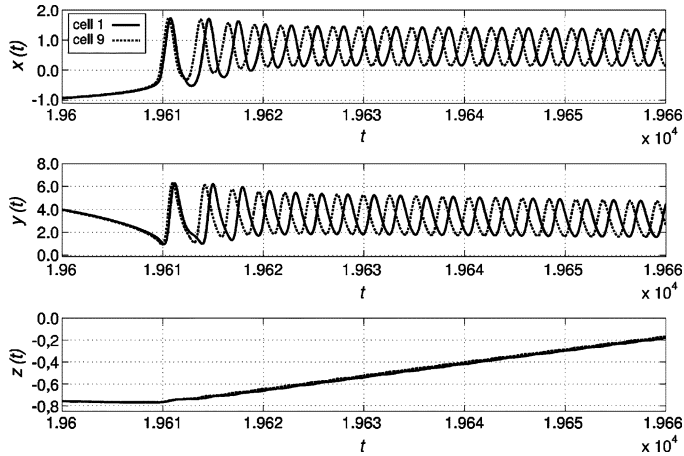


Fig. 9. Enlargement of the state evolution, after the transient, of two cells of the network whose topology is reported in Fig. 6(b): the solid line refers to cell 1 and the dotted line to cell 9.

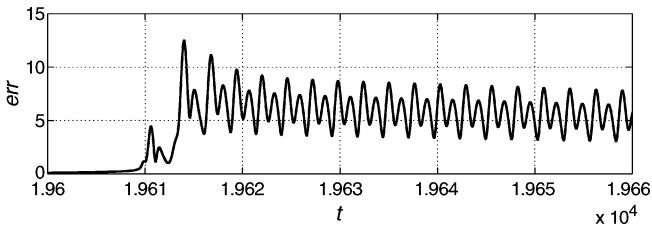


Fig. 10. Enlargement of the global error of the evolution of the network whose topology is reported in Fig. 6(b) in the same time interval used in Fig. 9.

the cells synchronize because the global error converge to zero. Furthermore, since $g_s k = 1.2861$, the time evolution shows oscillations on burst, as predicted by the bifurcation diagram of Fig. 2. The second network is characterized by the topology shown in Fig. 6(b) in which the cells are numbered following the same rule used for the previous example. The three largest eigenvalues of the associated adjacency matrix are $\lambda_1 = 3.0$, $\lambda_2 = \lambda_3 = 2.7093$. It follows that the considered network should not synchronize because $g_s \lambda_2 \simeq 1.161 > \bar{\alpha} \simeq 1.06$. In fact, the states of the cells do not synchronize as evidenced by Figs. 9 and 10. These figures show the evolution, after a sufficient long transient, of the state x of cells 1 and 9, respectively, and the corresponding global error in a suitable time interval to point out the differences. In conclusion, networks belonging to the same class and with the same coupling strength may behave differently, depending on their topology, that still influences synchronization properties.

VII. CONCLUSION

In this work, using the technique due to Pecora and Carroll, based on the MSE and the MSF, we have investigated the existence of synchronous states and the bifurcation diagram of networks of synaptically coupled neurons described by the HR model. In a quite natural way, the bifurcation parameter, used for both the generation of a modified MSF and the bifurcation diagram, turns out to be the product of the coupling strength g_s by the node degree k . Through the analysis of the bifurcation diagram and of the modified MSF as the bifurcation parameter is varied, the different dynamics of the possible synchronous states have been evidenced. Furthermore, the influence of the topology on the synchronization properties of the network has been shown through an example.

REFERENCES

- [1] X.-J. Wang and J. Rinzel, "Oscillatory and bursting properties of neurons," in *Handbook of Neural Networks and Brain Function*, M. Arbib, Ed. Cambridge, MA: MIT Press, 1995, pp. 686–691.
- [2] W. Singer and C. M. Gray, "Visual features integration and the temporal correlation hypothesis," *Annual Rev. Neurosci.*, vol. 18, pp. 555–586, 1995.
- [3] P. R. Roelfsema, A. K. Engel, P. Knig, and W. Singer, "Visuomotor integration is associated with zero time-lag synchronization among cortical areas," *Nature*, vol. 385, pp. 157–161, 1997.
- [4] E. Rodriguez, N. George, J.-P. Lachaux, J. Martinerie, B. Renault, and F. J. Varela, "Perception's shadow: Long-distance synchronization of human brain activity," *Nature*, vol. 397, pp. 430–433, 1999.
- [5] W. T. Oud and I. Tyukin, "Sufficient conditions for synchronization in an ensemble of Hindmarsh and Rose neurons: Passivity-based approach," in *Proc. IFAC NOLCOS 2004*, Stuttgart, Germany, 2004, pp. 1–3.
- [6] I. Belykh, E. de Lange, and M. Hasler, "Synchronization of bursting neurons: What matters in the network topology," *Phys. Rev. Lett.*, vol. 94, no. 13, pp. 188101(1)–188101(4), May 2005.
- [7] J. L. Hindmarsh and R. M. Rose, "Model of neuronal bursting using three coupled first order differential equations," *Proc. Royal Soc. B*, vol. 221, no. 1222, pp. 87–102, Mar. 1984.
- [8] G. X. Qi, H. B. Huang, H. J. Wang, X. Zhang, and L. Chen, "General conditions for synchronization of pulse-coupled bursting neurons in complex networks," *Europhys. Lett.*, vol. 74, no. 4, pp. 733–739, 2006.
- [9] P. Checco, M. Righero, M. Biey, and L. Kocarev, "Information processing in networks of coupled Hindmarsh-Rose neurons," in *Proc. NOLTA 2006*, Bologna, Italy, 2006, pp. 671–674.
- [10] P. Checco, M. Biey, M. Righero, and L. Kocarev, "Synchronization and bifurcation in networks of coupled Hindmarsh-Rose neurons," in *Proc. ISCAS 2007*, New Orleans, LA, 2007, pp. 1541–1544.
- [11] L. M. Pecora and T. L. Carroll, "Master stability functions for synchronized coupled systems," *Phys. Rev. Lett.*, vol. 80, no. 10, pp. 2109–2112, Mar. 1998.
- [12] J. L. Hindmarsh and P. Cornelius, "The development of the Hindmarsh-Rose model for bursting," in *Bursting: The Genesis of Rhythm in the Nervous System*, S. Coombes and P. Bressloff, Eds. Singapore: World Scientific, 2005, ch. 1, pp. 3–18.
- [13] E. M. Izhikevich, "Which model to use for cortical spiking neurons?," *IEEE Trans. Neural Netw.*, vol. 15, no. 5, pp. 1063–1070, Sep. 2004.
- [14] M. Bazhenov, R. Huerta, M. I. Rabinovich, and T. Sejnowski, "Cooperative behavior of a chain of synaptically coupled chaotic neurons," *Physica D*, vol. 116, no. 3–4, pp. 392–400, Jun. 1998.
- [15] P. Checco, M. Biey, and L. Kocarev, "Synchronization in random networks with given expected degree sequences," *Chaos, Solitons, Fractals*, vol. 35, no. 3, pp. 562–577, Feb. 2008.
- [16] A. Wolf, J. B. Swift, H. L. Swinney, and J. A. Vastano, "Determining Lyapunov exponents from a time series," *Physica D*, vol. 16, pp. 285–317, 1985.
- [17] M. Fiedler, "Algebraic connectivity of graphs," *Czech. Math. J.*, vol. 23, no. 98, pp. 298–305, 1973.